

WEAK INTER MOLECULAR INTERACTIONS: CRYSTAL STRUCTURE AND HIRSHFELD SURFACE ANALYSIS

Dipak K. Hazra

Department of Physics, Uluberia College, Uluberia, Howrah -711315, India.

Abstract: The crystal structure of 4-chloro-1H-pyrrolo [2,3-b] pyridine (1) has been determined from single crystal X-ray analysis at 100 K. In the crystal packing intermolecular N-H...N and C-H...Cl interactions forming $R_2^2(8)$ and $C_1^1(6)$ graph-set motif. The relative contributions of different interactions to the Hirshfeld surface in (I) are dominantly H...H, Cl...H, C...H and N...H types which can account for 55-85% of the total Hirshfeld surface area.

Key words– Crystal structure, Weak inter molecular interactions, Hirshfeld surface analysis.

1. INTRODUCTION

Intermolecular interactions, especially hydrogen bonds, have been a topic of wide scientific interest due to their role in crystal engineering and biological recognition processes [1,2]. Among the different hetero atoms, nitrogen (N), oxygen (O), sulfur (S) and halogen-substituted phenyl derivatives (Cl, Br) are the most common in organic compounds. Many of the synthons identified so far in supramolecular chemistry involve N...H/N, N...H/O, O...H/N and O...H/O hydrogen bonds, which provide the requisite robustness and reproducibility to create new solid-state structures [3–5]. In addition to these relatively strong hydrogen bonds, weak interactions such as C...H/ acceptor (O, N) are also important in describing the self assembly process. In this context, the chlorine atom with its low electronegativity has been labelled as a weak acceptor,6 and its acceptor potential usually overlooked. While the weak O...H/Cl and N...H/Cl interactions are considered as hydrogen bonds, the nature of even weaker C...H/Cl interactions is not yet fully understood [7,8]. In the last few years the analysis of molecular crystal structures using tools based on Hirshfeld surfaces has rapidly gained in popularity. This approach represents an attempt to represents the internuclear distances and angles, crystal packing diagrams with molecules represented via various models, and the identification of close contacts deemed to be important [9].

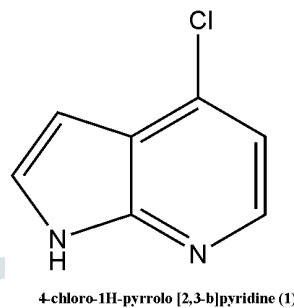
In order to explore the interplay of such strong and weak interactions in supramolecular assembly, we revisit the structures [10] determined by single crystal structure study along with Hirshfeld surface analysis to quantitatively visualize various intermolecular interactions.

2: EXPERIMENTAL SECTION

2.1: Data collection and Structure determination

The compound, 4-chloro-1H-pyrrolo [2,3-b] pyridine (1), was purchased from Aldrich, NY, USA (CAS Nos. 55052-28-3), and used without further purification. Good quality single crystals were obtained from methanol (CH₃OH) solvent by slow evaporation at room temperature. A colorless single crystal of dimensions ca. 0.40 x 0.30 x 0.25 mm³ was selected for the X-ray diffraction experiment. Intensity data were collected on a Bruker SMART APEX CCD X-ray diffractometer using graphite-monochromated MoK α radiation

($\lambda = 0.7107\text{\AA}$). The crystal was cooled to 100(2) K with a liquid nitrogen stream using an Oxford cryosystem. The crystal-to-detector distance was fixed to 40 mm and the scan width per frame ($\Delta\omega$) was 0.3° . The Lorentz-polarization correction and the integration of the diffracted intensities were performed using the SAINT [11] program, while an empirical absorption correction was applied using the SADABS [12] program. The crystal structure was redetermined by direct methods using SHELXS97 [13] and refined in the spherical-atom approximation (based on F^2) by using SHELXL97 [13] with anisotropic displacement parameters for all non-hydrogen atoms. The positions of H-atoms were located from the difference Fourier maps and refined with isotropic thermal parameters. A summary of crystal data and relevant refinement parameters for compound is provided in Table 1.



2. 2: Hirshfeld Surface Analysis

Hirshfeld Surfaces [30-32] and the associated 2D-fingerprint plots [14-16] were calculated using CrystalExplorer [17]. Bond lengths to hydrogen atoms were set to typical neutron values (C-H=1.083 \AA and N-H=1.030 \AA). For each point on the Hirshfeld isosurface, two distances d_e , the distance from the point to the nearest nucleus external to the surface, and d_i , the distance to the nearest nucleus internal to the surface, are defined. The normalized contact distance (d_{norm}) based on d_e and d_i is given by

$$d_{\text{norm}} = \frac{(d_i - r_i^{\text{vdw}})}{r_i^{\text{vdw}}} + \frac{(d_e - r_e^{\text{vdw}})}{r_e^{\text{vdw}}}$$

, where r_i^{vdw} and r_e^{vdw} being the van der Waals radii of the atoms. The value of d_{norm} is negative or positive depending on intermolecular contacts being shorter or longer than the van der Waals separations. The parameter d_{norm} displays a surface with a red-white-blue color scheme, where bright red spots highlight shorter contacts, white areas represent contacts around the van der Waals separation, and blue regions are devoid of close contacts.

Table 1: Experimental details: Crystal data, structure solution and refinement parameters of $\text{C}_7\text{H}_5\text{N}_2\text{Cl}$ (1) .

Empirical formula	$\text{C}_7\text{H}_5\text{N}_2\text{Cl}$
Formula weight	152.58
Wavelength (\AA)	0.71073
Crystal system	Monoclinic
Temperature (K)	100(2)
Space group	$P2_1/n$
a, b, c (\AA)	5.2586(2), 8.9160(3), 13.8165(5)
β ($^\circ$)	90.500(2)
Volume (\AA^3)	647.77(4)
Z	4
Absorption coefficient (mm^{-1})	0.495
F(000)	312
θ range ($^\circ$), ($\sin \theta/\lambda$) $_{\text{max}}$ (\AA^{-1})	2.72 to 50.31, 1.08
Completeness to 2θ (%)	98.2
Refinement method	Full-matrix least-squares on F^2
Final R indices [$I > 2\sigma(I)$]	$R_1 = 0.0543$, $wR_2 = 0.1268$
R indices (all data)	$R_1 = 0.0617$, $wR_2 = 0.1297$
Largest diff. peak and hole (e. \AA^{-3})	1.799 and -0.249

3: RESULTS AND DISCUSSION

3.1: Crystal and molecular structure

An ORTEP diagram of molecule (1) with atom labeling scheme and thermal ellipsoids at the 40% probability level is shown in Fig. 1. The molecule is essentially planar with an r.m.s. deviation of 0.012Å for the non-hydrogen atoms defining the least-squares plane.

In addition to van der Waals interactions, the crystal packing in the title compound is stabilized by intermolecular N-H...N and C-H...Cl hydrogen bonds (Table 2). A pair of intermolecular N-H...N hydrogen bonds with the pyrrole N1 atom in the molecule at (x,y,z) acting as a donor to the pyridine N2 atom in the molecule at (2-x, -y, 1-z) generates a centrosymmetric dimeric unit forming a $R_2^2(8)$ graph-set motif [43]. Similarly, the intermolecular C1-H1...Cl1 hydrogen bonds connect the molecules of (1) into one-dimensional polymeric chain of $C_1^1(6)$ motif propagating along the [010] direction. The combination of $R_2^2(8)$ rings and $C_1^1(6)$ chains results into a two-dimensional molecular framework built with fused $R_4^4(30)$ rings in the (011) plane (Fig. 2).

Table 2: Intermolecular contacts (Å, °) in $C_7H_5N_2Cl$ (1).

D—H...A	d(D—H)	d(H...A)	d(D...A)	D—H...A
N(1)—H(1N)...N(2) ⁱ	0.88(2)	2.02(2)	2.896(1)	174.6(19)
C(1)—H(1)...Cl(1) ⁱⁱ	0.98(2)	2.94(2)	3.832(1)	152.5(12)

Symmetry codes: (i) -x+2,-y,-z+1 (ii) -x+3/2,+y-1/2,-z+1/2.

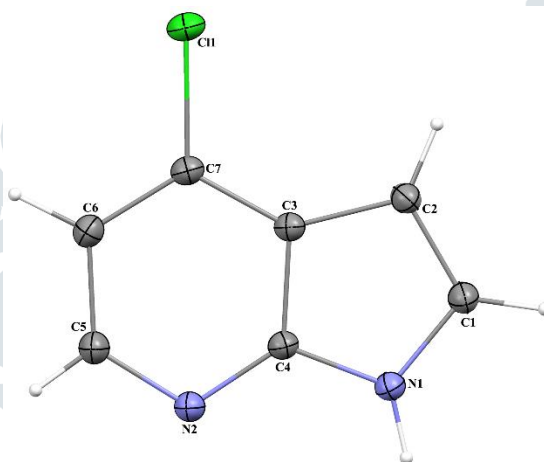


Fig. 1: An ORTEP view and atom numbering scheme of (1) with displacement ellipsoids at the 40% probability level. Hydrogen atoms are shown as small spheres of arbitrary radii.

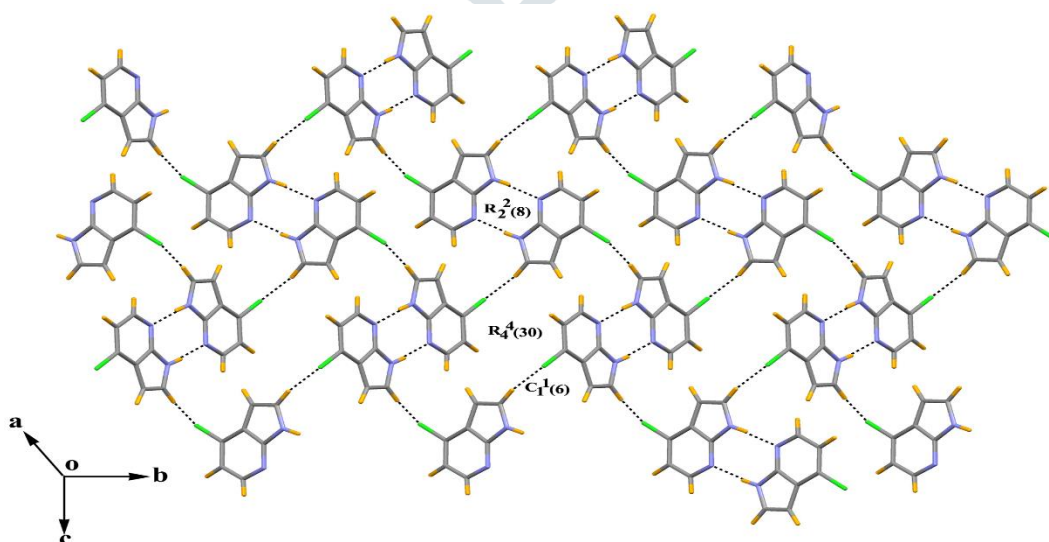


Fig. 2: Formation of two-dimensional framework built with fused $R_4^4(30)$ rings in the (011) plane for $C_7H_5N_2Cl$ (1).

3.2: Hirshfeld surface Analysis

The Hirshfeld surface of the title compound is illustrated in Fig. 3(i), showing surface that has been mapped over d_{norm} range of -0.5 to 1.0 Å. The dominant interactions between the pyrrole N-H and pyridine N atoms forming a dimeric unit in (**1**) can be seen as bright red areas (marked as **a** and **b**) on the Hirshfeld surface (Fig. 3(i)). The light red spots labelled as **c** and **d** in Fig. 3(i) are due to C-H...Cl contacts. In the 2D fingerprint plot, Fig. 3(ii), a pair of sharp spikes of almost equal length in the region $1.9 < d_e + d_i < 2.7$ Å are characteristics of a cyclic hydrogen bonded $R^2_2(8)$ synthon [18]. The points in the (d_i, d_e) regions of (1.6, 1.2 Å) and (1.2, 1.6 Å) in Fig. 3(ii) are due to N1-H1...N2 interactions. The upper spike **a** in Fig. 3(ii) corresponds to a donor spike (the pyrrole H-atom interacting with the N-atom of the pyridine ring), the lower spike **b** being an acceptor spike (N-atom of the pyridine moiety interacting with the H atom of the pyrrole ring). The wings in the region of $d_i = 1.1$ Å to $d_e = 1.7$ Å and $d_e = 1.1$ Å to $d_i = 1.7$ Å, marked as **c** and **d** in Fig. 3(ii), correspond to H...Cl interactions in the title compound. Even though the N...H interactions are shortest and most likely the strongest in the title compound, they cover only about 12% of the Hirshfeld surface area, whereas the contributions of the H...Cl and H...H interactions are 20% and 31%, respectively. The relative contribution of different interactions to the Hirshfeld surface was calculated for (**1**) as well as a number of chloropyridines fused to a pyrrole or a phenyl ring system (Fig. 4) available in the CSD. Due to varying the number and the types of substituents on the monochloro bicyclic systems, they are not directly comparable across the compounds, but it offers some insight into possible intermolecular contacts in this class of compounds. No significant Cl...Cl interactions are observed, with Cl...H close contacts varying from 6.6% in AJETAL [19] to 19.7% in (**1**). Fig. 4, indicates that the molecular interactions in these compounds are dominantly H...H, Cl...H, C...H and N...H types, which can account for 55-85% of the Hirshfeld surface area.

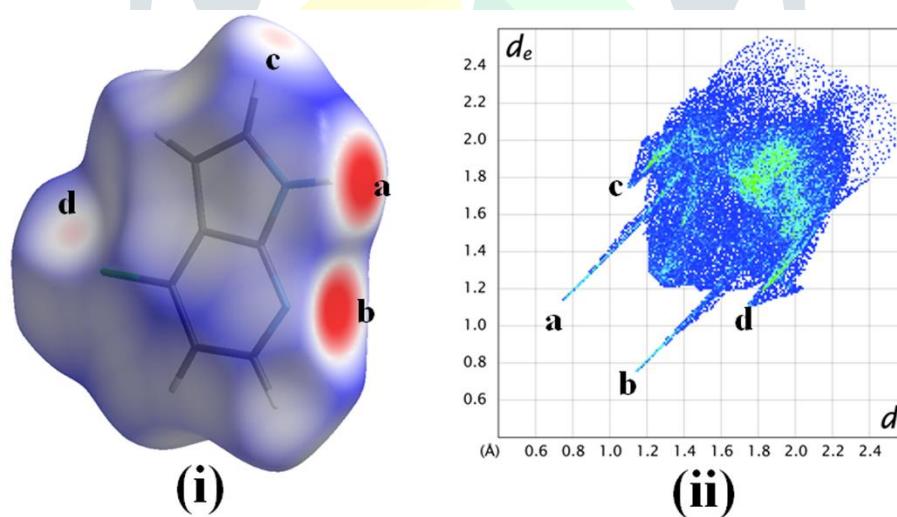


Fig. 3: (i) Hirshfeld surface (ii) 2D-fingerprint plot for $C_7H_5N_2Cl$ (**1**).

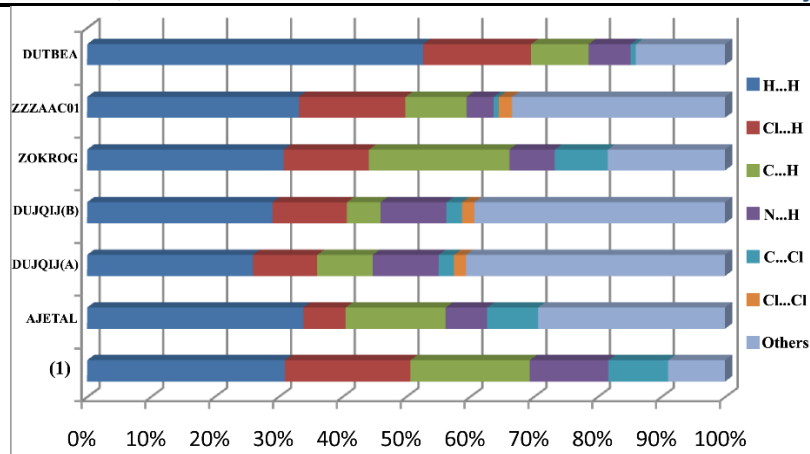


Fig. 4: Relative contribution of different interactions to the Hirshfeld surface area of selected chloropyridine compounds.

4: CONCLUSIONS

The results of the structure analysis based on high resolution ($d=0.46\text{\AA}$) X-ray diffraction data and the Hirshfeld surface analysis of a chloropyrrolo-pyridine have been used to highlight the electronic feature of the molecule, the types of intermolecular interactions and, specially, to provide the information about the acceptor potentiality of the chlorine atom. A careful evaluation leads to a clear understanding of the nature of intermolecular N-H...N and C-H...Cl interactions in terms of three-dimensional network. While the N-H...N interaction can be classified as a moderately strong hydrogen bond, the C-H...Cl contact can be represented as a weak “closed-shell” interaction. The directionality of the C-H...Cl interaction in the present structure plays an important role in generating as well as stabilizing the supramolecular structure.

ACKNOWLEDGEMENTS

The author is grateful to Prof. A. Mukherjee and Prof. M. Mukherjee for many useful discussions in connection with the field of research described in this article.

References

1. G. R. Desiraju, *Crystal Engineering. The Design of Organic Solids*; Elsevier: New York, (1989).
2. G. A. Jeffrey and W. Saenger, *Hydrogen Bonding in Biological Structures*, Springer, Berlin, (1991).
3. G.R. Desiraju, *Nature* **412** (2001) 397.
4. F. H. Allen, W. D. S. Motherwell, P. R. Raithby, G. P. Shields, R. Taylor, *New J. Chem.* **23** (1999) 25.
5. V. Sethuraman, N. Stanley, P. T. Muthiah, W. S. Sheldrick, M. Winter, P. Luger, M. Weber, *Cryst. Growth Des.* **3** (2003) 823.
6. V. R. Hathwar, T. N. Guru Row, *J. Phys. Chem. A* **114** (2010) 13434.
7. D. J. R. Duarte, M. M. de las Vallejos, N. M. Peruchena, *J. Mol. Model.* **16** (2010) 737.
8. N. J. M. Amezaga, S. C. Pamies, N. M. Peruchena, G. L. Sosa, *J. Phys. Chem. A* **114** (2010) 552.
9. M. A. Spackman, D. Jayatilaka, *CrystEngComm.* **11** (2009) 19.
10. D. K. Hazra, A. K. Mukherjee, M. Helliwell, M. Mukherjee *CrystEngComm*, **14**, (2012) 993
11. APEX2, SAINT and XPREP. Bruker AXS Inc., Madison, Wisconsin, USA, (2007).
12. SADABS. Bruker AXS Inc., Madison, Wisconsin, USA, (2001).
13. G. M. Sheldrick, *Acta Crystallogr. Sect. A* **64** (2008) 112.
14. A. L. Rohl, M. Moret, W. Kaminsky, K. Claborn, J. J. McKinnon, B. Kahr, *Cryst. Growth Des.* **8** (2008) 4517.
15. A. Parkin, G. Barr, W. Dong, C. J. Gilmore, D. Jayatilaka, J. J. McKinnon, M. A. Spackman, C. C. Wilson, *CrystEngComm.* **9** (2007) 648.
16. M. A. Spackman, J. J. McKinnon, *CrystEngComm.* **4** (2002) 378.

17. S. K. Wolff, D. J. Grimwood, J. J. McKinnon, D. Jayatilaka, M. A. Spackman, Crystal Explorer 2.0; University of Western Australia: Perth, Australia, (2007). <<http://hirshfeldsurfacenet.blogspot.com/>>.
18. B. Chattopadhyay, A. K. Mukherjee, N. Narendra, H. P. Hemantha, V. V. Sureshbabu, M. Helliwell, M. Mukherjee, Cryst. Growth Des. **10** (2010) 4476.
19. R. Selig, D. Schollmeyer, W. Albrecht, S. Laufer, Acta Crystallogr. Sect. E **65** (2009) o3018.

